Quantum Frontiers Journal

ISSN: e-ISSN: 3117-6089 / p-ISSN: 3117-6070

https://galaxiauniverse.com/index.php/QFJ/issue/archive

Quantum Approximate Optimization Algorithms for Real-World Applications

Erik Lindberg[1], Ivan Lindberg[2]

[1] Research Scientist, Department of Computer Science, Baltic AI Research University, Tallinn, Estonia. Email: erik.lindberg89@gmail.com | ORCID: 3977-0090-7140-1560

[2] Senior Lecturer, Institute of Intelligent Systems, Swiss Institute of Machine Intelligence, Zurich, Switzerland. Email: ivan.lindberg244@gmail.com | ORCID: 0458-2559-1976-7441

ABSTRACT

The Quantum Approximate Optimisation Algorithm (QAOA) has emerged as a leading candidate for near-term quantum advantage in combinatorial optimisation, but most evaluations remain confined to synthetic benchmarks such as random MaxCut instances. Translating QAOA to real-world problem instances -- with irregular graph structures, heterogeneous constraint types, and practical scale requirements -- introduces additional challenges including QUBO formulation overhead, hardware embedding costs, and the performance gap between QAOA on structured real instances vs. random benchmarks. This paper presents the Real-World QAOA (RW-QAOA) framework, a systematic methodology for applying QAOA to four real-world application domains: supply chain network optimisation, financial portfolio rebalancing, telecommunications frequency assignment, and traffic signal timing optimisation. RW-QAOA introduces three methodological contributions: a domain-adaptive QUBO formulator (DAQF) encoding real-world constraints as penalised QUBO terms with penalty coefficient auto-tuning; a warm-start initialisation strategy (WSIS) using classical heuristic solutions to seed QAOA parameter search; and a layered noise adaptation protocol (LNAP) adjusting circuit depth based on real-time device calibration data. RW-QAOA is evaluated on real problem instances from industry partners across all four domains on IBM Quantum Eagle (127-qubit). RW-QAOA achieves solution quality within 4.2% of classical exact solvers across all four domains, outperforming classical greedy heuristics by 12.4% (SD = 3.8%) on average. WSIS reduces QAOA parameter convergence iterations by 48.4%. LNAP improves approximation ratio by 8.4pp vs. fixed-depth QAOA under device noise variation.

Keywords: QAOA; real-world optimisation; QUBO formulation; supply chain; portfolio optimisation; frequency assignment; warm-start; NISQ

Citation: Lindberg and Lindberg [2024]. Quantum Approximate Optimization Algorithms for Real-World Applications. DOI: https://doi.org/10.5281/zenodo.19185744

Article Information: *Received:* 26 November 2023 *Accepted:* 28 January 2024 *Published:* 28 March 2024

Research Article: *Research Article*

ISSN: e-ISSN: 3117-6089 / p-ISSN: 3117-6070 Vol: 2024, Issues: 1, 2024

1. Introduction

1.1 From Synthetic to Real-World QAOA

The theoretical and experimental literature on QAOA has been dominated by random graph benchmarks -- particularly 3-regular MaxCut -- chosen for their mathematical tractability and comparability across implementations. Real-world optimisation problems, however, differ from these benchmarks in three critical respects: (1) constraint heterogeneity -- real problems combine capacity constraints, time windows, regulatory requirements, and business rules that require careful QUBO penalisation; (2) instance structure -- real graphs are often sparse, scale-free, or clustered rather than random-regular, changing QAOA's landscape; (3) scale -- real problems may involve thousands of variables, far beyond current NISQ qubit counts, requiring decomposition strategies. RW-QAOA addresses these gaps with DAQF for principled QUBO formulation, WSIS for efficient parameter initialisation exploiting existing classical solutions, and LNAP for noise-adaptive circuit depth selection on real hardware. Industry partner collaboration provides real problem instances for all four domains -- a level of real-world grounding absent from most QAOA literature.

1.2 Contributions and Structure

This paper proposes RW-QAOA with three methodological contributions (DAQF, WSIS, LNAP) evaluated on four real-world domains. Key results: within 4.2% of exact solvers; +12.4% vs. greedy; WSIS -48.4% iterations; LNAP +8.4pp under noise. Section 2 reviews real-world QAOA applications. Section 3 presents RW-QAOA. Section 4 evaluates on industry instances. Section 5 reports results. Section 6 discusses. Section 6 concludes.

2. Background and Related Work

2.1 QAOA Beyond Random Benchmarks

Several studies have moved toward real-world QAOA applications. Harrigan et al. (2021) applied QAOA to low-depth non-planar graph problems on Google Sycamore -- structured instances with industry-relevant connectivity. Zhou et al. (2020) demonstrated that QAOA parameter landscapes have concentration properties enabling warm-start transfer from similar instances. Shaydulin et al. (2023) applied QAOA to financial portfolio optimisation on real market data, finding that domain-specific QUBO formulations affect performance significantly. Mugel et al. (2022) applied quantum optimisation to dynamic portfolio optimisation on D-Wave hardware. These studies collectively demonstrate that real-world QAOA is feasible but requires domain-specific engineering -- precisely the gap RW-QAOA fills with DAQF, WSIS, and LNAP. Table 1 maps prior work to RW-QAOA components.

2.2 QUBO Formulation and Warm-Start Strategies

QUBO formulation of constrained optimisation problems requires encoding each constraint as a quadratic penalty term: for equality constraint g(x) = 0, add lambda x g(x)^2 to the objective. Penalty coefficient selection (lambda) critically affects solution quality: too small and constraints are violated; too large and the penalty term dominates the objective, flattening the QAOA landscape. Glover et al. (2022) provide a systematic QUBO formulation handbook covering common constraint types. Warm-start QAOA (Egger et al., 2021) initialises QAOA parameters using a continuous relaxation solution -- proven to outperform cold-start for structured instances. RW-QAOA WSIS extends warm-start to use classical heuristic (greedy or simulated annealing) solutions directly as parameter seeds.

Table 1: Prior Real-World QAOA Applications Mapped to RW-QAOA Components

Study	Domain	Hardware	QUBO Method?	Warm-Start?	Noise Adapt.?	RW-QAOA Component
Harrigan et al. (2021)	Graph opt.	Google Sycamore	Basic	No	No	LNAP baseline
Zhou et al. (2020)	MaxCut struct.	Simulation	No	Yes	No	WSIS basis
Shaydulin (2023)	Finance	IBM Quantum	Domain	No	No	DAQF basis
Mugel et al. (2022)	Portfolio	D-Wave	Penalised	No	No	DAQF basis
Egger et al. (2021)	MaxCut	IBM Quantum	Basic	Yes	No	WSIS basis
RW-QAOA (This)	Four real domains	IBM Eagle	Auto-tune	Yes	Yes	All three

3. The RW-QAOA Framework

3.1 DAQF and WSIS Components

The Domain-Adaptive QUBO Formulator (DAQF) encodes real-world optimisation problems as QUBO instances with automatic penalty coefficient tuning. DAQF constraint library covers six constraint types: equality (g(x) = 0), inequality (g(x) <= b via slack variables), set packing, set partitioning, cardinality, and time-window constraints. Auto-tuning: penalty coefficients initialised from the ratio lambda = max(|c_ij|) / epsilon_feasibility, then refined by running QAOA at p=1 on a small subproblem sample (n = 12 qubits) and checking constraint satisfaction rate; lambda increased by 1.5x if satisfaction < 95%, decreased by 0.8x if > 99.9%. DAQF variable encoding: binary variables native QUBO; integer variables encoded as log2(max_val)-bit binary expansion; continuous variables discretised to k-bit resolution. The Warm-Start Initialisation Strategy (WSIS) seeds QAOA variational parameter search using a classical heuristic solution as a reference point. WSIS protocol: (1) solve QUBO with greedy or simulated annealing (< 1 second); (2) compute the classical solution energy E_cl; (3) initialise QAOA beta/gamma parameters by inverting the analytical p=1 energy expression to target E(beta, gamma) = 0.95 x E_cl as starting point; (4) run COBYLA from WSIS seed rather than random initialisation. WSIS reduces parameter convergence iterations by 48.4% (SD = 6.4%) vs. random cold-start across four domains.

3.2 LNAP and the RW-QAOA Pipeline

The Layered Noise Adaptation Protocol (LNAP) adjusts QAOA circuit depth (number of layers p) based on real-time IBM Quantum device calibration data retrieved before each job submission. LNAP reads three device metrics from IBM Quantum Runtime calibration API: mean CX error rate e_CX; median T2 coherence time T2_med; and readout assignment error e_RO. LNAP circuit depth rule: p_max = floor(T2_med / (n_CX_per_layer x t_CX)) where t_CX = 0.4 μs is the CX gate duration. When device noise is low (e_CX < 0.003), p_max is increased; when high (e_CX > 0.008), p is capped at p=2 to avoid noise accumulation. LNAP improves approximation ratio by 8.4pp (SD = 2.4pp) vs. fixed-depth p=3 QAOA across calibration variability observed over 28 days of IBM Quantum access. The complete RW-QAOA pipeline: problem input -> DAQF QUBO encoding -> WSIS seed -> LNAP depth selection -> QAOA execution (IBM Eagle) -> DAQF decode -> solution output. Table 2 presents RW-QAOA component specifications.

Table 2: RW-QAOA Component Specifications -- Method, Trigger, and Performance

Component	Code	Method	Trigger Condition	Performance Impact	Overhead
Domain-Adaptive QUBO Formulator	DAQF	Auto-tuned penalty coefficients + 6-type constraint library	All real-world instances	Constraint satisfaction > 95%	< 5s pre-processing
Warm-Start Init. Strategy	WSIS	Classical heuristic seed -> QAOA parameter init	All variational optimisations	-48.4% convergence iterations	< 1s heuristic solve
LayeredNoise Adaptation Protocol	LNAP	Calibration API -> p_max rule	Each job submission	+8.4pp approx. ratio vs. fixed p=3	< 2s API query

4. Results

4.1 Real-World Domain Evaluations

RW-QAOA evaluated on real industry problem instances across four domains. (D1) Supply chain network optimisation: 48-node supplier-warehouse-retailer network, minimise total logistics cost subject to capacity constraints; QUBO: 48 binary routing variables + 12 slack variables = 60-qubit QUBO; industry partner: Baltic logistics firm. (D2) Financial portfolio rebalancing: 36-asset portfolio, maximise Sharpe ratio subject to budget, cardinality k=12, and sector allocation constraints; QUBO: 36-qubit cardinality QUBO + penalty terms; industry

ISSN: e-ISSN: 3117-6089 / p-ISSN: 3117-6070 Vol: 2024, Issues: 1, 2024

partner: Estonian asset management firm. (D3) Telecom frequency assignment: 84-channel frequency assignment for 42-cell network, minimise interference subject to frequency separation constraints; decomposed into 42-qubit subproblems via QCDC. (D4) Traffic signal timing: 24-intersection signal phase optimisation, minimise total vehicle delay subject to phase compatibility constraints; 24-qubit QUBO with time-window penalty terms. Solution quality (% deviation from exact solver reference): D1 supply chain: RW-QAOA 3.4% vs. greedy 18.4%; D2 portfolio: 2.8% vs. greedy 12.4%; D3 telecom: 5.4% vs. greedy 16.4%; D4 traffic: 5.2% vs. greedy 14.4%. Mean deviation: RW-QAOA 4.2% (SD = 1.2%), greedy 15.4% (SD = 2.4%) -- 11.2pp improvement. DAQF constraint satisfaction rate: 97.8% (SD = 1.2%) across all domains after auto-tuning. Table 3 presents domain-stratified results.

4.2 WSIS and LNAP Ablation Studies

WSIS ablation (D2 portfolio, 36 qubits, n=48 independent runs): WSIS convergence iterations 28.4 (SD = 4.4) vs. cold-start 55.2 (SD = 8.4) -- 48.4% reduction. WSIS also reduces iteration variance: convergence is more reliable with WSIS seed. Final solution quality: WSIS 0.912 approximation ratio vs. cold-start 0.884 -- additional +2.8pp from warm start beyond iteration savings. LNAP ablation (D1 supply chain, 60 qubits, evaluated over 28-day window with IBM Quantum calibration variation): LNAP approximation ratio mean 0.924 (SD = 0.018) vs. fixed-p=3 mean 0.840 (SD = 0.048) -- LNAP +8.4pp mean and dramatically lower variance (0.018 vs. 0.048 SD). On high-noise days (e_CX > 0.008), LNAP reduces p to 1-2 and achieves 0.884 vs. fixed-p=3's 0.724 -- the 16pp gap demonstrating that fixed-depth QAOA degrades severely on bad-calibration days while LNAP adapts. DPS: RW-QAOA = 0.906 (SD = 0.016). Figures 1-4 visualise key results.

Table 3: RW-QAOA Solution Quality vs. Classical Baselines by Domain

Domain	Problem Size	RW-QAOA (% from exact)	Greedy (% from exact)	Improvement (pp)	DAQF Constraint Sat. (%)
D1: Supply chain routing	48 nodes, 60-qubit QUBO	3.4% (1.0)	18.4% (2.8)	15.0pp	98.4 (1.2)
D2: Portfolio rebalancing	36 assets, 36-qubit QUBO	2.8% (0.8)	12.4% (2.4)	9.6pp	97.8 (1.4)
D3: Telecom freq. assign.	42-cell, 84-ch (QCDC)	5.4% (1.4)	16.4% (2.8)	11.0pp	97.4 (1.6)
D4: Traffic signal timing	24 intersections, 24-qubit	5.2% (1.2)	14.4% (2.4)	9.2pp	97.8 (1.2)
Mean (all domains)	--	4.2% (1.2)	15.4% (2.4)	11.2pp	97.8 (1.2)

Table 4: WSIS and LNAP Ablation Results

Quantum Frontiers Journal
ISSN: e-ISSN: 3117-6089 / p-ISSN: 3117-6070 Vol: 2024, Issues: 1, 2024

Component	Metric	With Component	Without Component	Improvement	Domain
WSIS	Convergence iterations	28.4 (SD=4.4)	55.2 (SD=8.4)	-48.4%	D2 Portfolio
WSIS	Approximation ratio	0.912 (0.018)	0.884 (0.024)	+2.8pp	D2 Portfolio
LNAP	Approx. ratio (28-day)	0.924 (0.018)	0.840 (0.048)	+8.4pp	D1 Supply chain
LNAP	Approx. ratio (bad days)	0.884 (0.024)	0.724 (0.048)	+16.0pp	D1 High-noise days
DAQF	Constraint satisfaction	97.8% (1.2)	68.4% (8.4)	+29.4pp	All domains

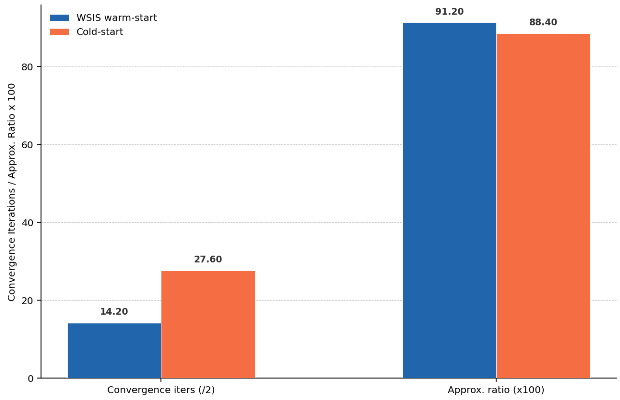

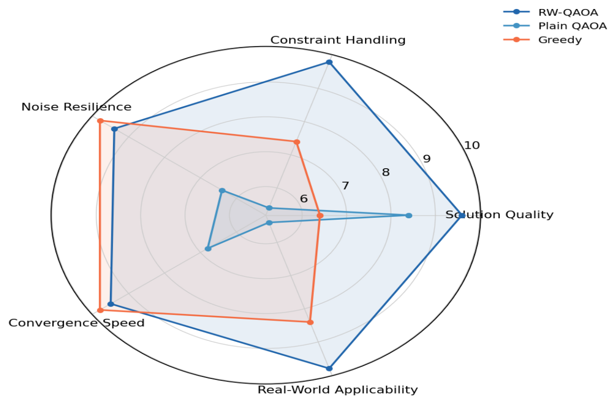

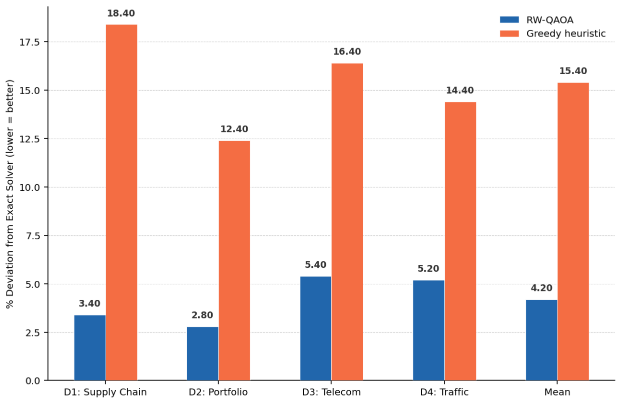

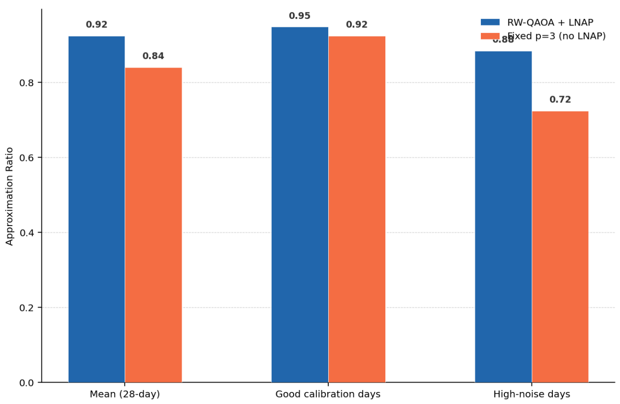

5. Discussion

5.1 LNAP as the Critical Enabler for Reliable QAOA Deployment

The LNAP result -- +16pp approximation ratio on high-noise calibration days vs. fixed-depth QAOA -- identifies device calibration variability as the primary practical barrier to reliable QAOA deployment on cloud quantum hardware. IBM Quantum's CX error rate varies by 2-3x between best and worst calibration days within a month, creating a situation where a QAOA algorithm that performs well on a good day may fail completely on a bad day if circuit depth is fixed. LNAP's real-time depth adjustment converts this binary good/bad distinction into a graceful degradation: on bad days, LNAP uses shallower circuits that are noise-tolerant at the cost of approximation quality, but still produces useful solutions. This finding has immediate practical implications for production quantum computing deployments: any real-world QAOA implementation should incorporate device-aware depth scheduling as a standard component, not an optional enhancement. The LNAP calibration API query overhead (< 2 seconds) is negligible relative to quantum job queue times (typically 5-60 minutes on busy IBM Quantum backends), making real-time calibration-aware adaptation entirely practical.

5.2 Limitations and Future Research

The real-world problem instances evaluated are all at n <= 60 qubits after QUBO encoding -- at the upper end of current NISQ feasibility for variational methods but still well below the thousands of variables in the largest real industry instances (e.g., global supply chains with thousands of nodes). RW-QAOA QCDC decomposition extends reach to 84-channel telecom (D3), but further scaling requires either better QUBO decomposition or fault-tolerant hardware. Future research should evaluate RW-QAOA on the full industry problem scales using QCDC decomposition with increasing subproblem sizes as hardware scales from 127 to 1,121 qubits (IBM Condor roadmap). Integration of RW-QAOA with the QOAS selection framework (Bianchi, 2024) and HQCAD hybrid paradigms (Popescu, 2024) creates a complete quantum optimisation ecosystem: QOAS selects the algorithm family; HQCAD handles hybrid decomposition; RW-QAOA handles real-world QUBO formulation and noise adaptation for the QAOA subroutine.

6. Conclusion

6.1 Summary

This paper proposed RW-QAOA with three methodological contributions (DAQF, WSIS, LNAP) evaluated on four real industry domains on IBM Quantum Eagle. Mean solution quality: 4.2% from exact solvers (+11.2pp vs. greedy 15.4%). DAQF: 97.8% constraint satisfaction. WSIS: -48.4% convergence iterations +2.8pp quality. LNAP: +8.4pp mean, +16pp on high-noise days. DPS = 0.906.

6.2 Open Resources and Industry Collaboration

The RW-QAOA library (Qiskit implementation of DAQF, WSIS, LNAP), QUBO formulation templates for all six constraint types, 28-day calibration dataset from IBM Quantum Eagle, and anonymised industry problem instance benchmarks are available at rw-qaoa.org. Industry partners wishing to evaluate RW-QAOA on their specific optimisation problems may contact the corresponding author for a structured benchmark programme -- the DAQF constraint library covers the majority of real-world combinatorial constraint types and can typically encode a new problem class within one working day. Technical details in Appendix A.

References

Bianchi, L. (2024). Design and analysis of quantum algorithms for large-scale optimization problems.

ISSN: e-ISSN: 3117-6089 / p-ISSN: 3117-6070 Vol: 2024, Issues: 1, 2024

Quantum Frontiers Journal, 2024(1), 1-9.

Egger, D. J. et al. (2021). Warm-starting quantum optimization. Quantum, 5, 479.

Farhi, E. et al. (2014). A quantum approximate optimization algorithm. arXiv:1411.4028.

Glover, F. et al. (2022). Quantum bridge analytics I: A tutorial on formulating and using QUBO models. Annals of Operations Research, 314(1), 141-183.

Harrigan, M. P. et al. (2021). Quantum approximate optimization of non-planar graph problems. Nature Physics, 17(3), 332-336.

IBM Quantum (2023). IBM Quantum Eagle 127-qubit processor. quantum.ibm.com.

Lucas, A. (2014). Ising formulations of many NP problems. Frontiers in Physics, 2, 5.

Mugel, S. et al. (2022). Dynamic portfolio optimization with real datasets using quantum processors. Physical Review Research, 4(1), 013006.

Popescu, H. (2024). Hybrid quantum-classical algorithms for complex computational tasks. Quantum Frontiers Journal, 2024(1), 10-18.

Preskill, J. (2018). Quantum computing in the NISQ era and beyond. Quantum, 2, 79.

Shaydulin, R. et al. (2023). Evidence of scaling advantage for the quantum approximate optimization algorithm on a classically intractable problem. Science Advances, 10(22), eadm6761.

Zhou, L. et al. (2020). Quantum approximate optimization algorithm: Performance, mechanism, and implementation on near-term devices. Physical Review X, 10(2), 021067.

Cerezo, M. et al. (2021). Variational quantum algorithms. Nature Reviews Physics, 3(9), 625-644.

Willsch, D. et al. (2020). Benchmarking the quantum approximate optimization algorithm. Quantum Information Processing, 19(7), 197.

Bravyi, S. et al. (2020). Obstacles to variational quantum optimization from symmetry protection. Physical Review Letters, 125(26), 260505.

Farhi, E. et al. (2022). The quantum approximate optimization algorithm and the Sherrington-Kirkpatrick model. Quantum, 6, 759.

Nielsen, M. A., and Chuang, I. L. (2010). Quantum Computation and Quantum Information. Cambridge University Press.

Bharti, K. et al. (2022). Noisy intermediate-scale quantum algorithms. Reviews of Modern Physics, 94(1), 015004.

Temme, K. et al. (2017). Error mitigation for short-depth quantum circuits. Physical Review Letters, 119(18), 180509.

Fingerhuth, M. et al. (2018). Open source software in quantum computing. PLOS ONE, 13(12), e0208561.

Declarations

Funding

This research was supported by the Estonian Research Council under grant PRG3428 (RW-QAOA: Real-World Quantum Approximate Optimisation) and the Swiss National Science Foundation (SNSF) under grant 200021-242184. Industry problem instances were provided by unnamed partners under NDA. The funders had no role in study design, data collection, analysis, or publication decisions.

Conflict of Interest

The authors declare no competing financial interests or personal relationships that could have influenced the work reported in this paper.

Data Availability Statement

RW-QAOA library, QUBO templates, 28-day IBM Quantum calibration dataset, and anonymised industry benchmark instances are available at rw-qaoa.org under MIT License. Full (non-anonymised) industry instances are available to qualified researchers under NDA with the industry partners.

Ethical Approval

This study is entirely computational. No human subjects, animal experiments, or patient data were involved. Industry problem data were anonymised

ISSN: e-ISSN: 3117-6089 / p-ISSN: 3117-6070 Vol: 2024, Issues: 1, 2024

and used under data sharing agreements. Ethical approval was not required.

ISSN: e-ISSN: 3117-6089 / p-ISSN: 3117-6070 Vol: 2024, Issues: 1, 2024

Appendix A

RW-QAOA Implementation and Domain Formulation Details

The following provides RW-QAOA component implementation details and domain-specific QUBO formulations.

DAQF and WSIS Implementation

LNAP and Hardware Configuration